Image Classification for Remote Sensing Data with Multi-Stage Approaches Using Inception V3 And Vgg16

Janarthanan.S[1, *], Dr. T. Ganesh Kumar[2]
[1,2] *School of Computing Science and Engineering, Galgotias University, India*
[1]*jana.mkce@gmail.com*, [2]*tganeshphd@yahoo.com*
Corresponding author: Janarthanan.S[1, *], [1]https://orcid.org/0000-0003-3003-6621

Abstract

The IRS P-6 LISS IV data set from an Indian remote sensing satellite with a high resolution multi-spectral camera with approximately 5.8m from an 817 km altitude Delhi image was primarily used in the main process of this image classification with a convolution neural network using deep learning model. The cropped image's classification of the sections necessitated the use of enhancing techniques, and the image size was 1000 megabytes. High-end software was required to open this picture file in order to view it. ERDAS imaging software viewer was initially employed for that purpose in order to crop images into the proper resolution pixels. Based on that cropped image, preprocessing for adding filters for improvement was utilized to classify images. Additionally, data from the group of items that were cropped was used to train the convolution neural network model using the example photos of the same pixels. Then, using the Jupyter notebook tool in Inception v3 and vgg16 with Tensorflow and a machine learning model, we had to use picture sample areas to train the model with learning rate and epoch rate to increase object detection accuracy.

Keywords: *Remote sensing, object detection, categorization, deep learning, machine learning, inception v3, vgg16*

1. Introduction

The first two categories in the introduction's access to this jupyter software's picture source are image enhancement and image categorization. The degree of image classification accuracy was then discussed.

1.1. Image Improvement

Image sensing is the collection of various data, including pictures, without any direct relationship to images. It is a technology or procedure that combines a number of sensors with digital photographs in order to measure distant geographic objects [1]. And it might be unique from several sensors and satellites. Additionally, several noise removal techniques have been used to images that have been received in order to enhance the image quality [2][3]. These images typically have issues with quality due to the use of various enhancement algorithms to produce a sharper and more contrasted brightness improvement technique from noise components.

In this work, the following techniques were employed to enhance the image resolution:

- Techniques utilizing the frequency and spatial domains
- Image enhancement

To enhance the image quality in the aforementioned areas, more filtering techniques are used.

The implementation of [4][5] for n x n improved the performance of the average filter and the 3 x 3 mask that are required for evaluation. In order to enhance and pre-process digital photographs further, the image features are improved in the image pre-processing programme [6][7]. For brightness pixels, comparable images with pixel damage were chosen. Additionally, using standard brightness, contrast, and sharpening, [9][10] the quality of the images used for remote sensing can be enhanced. After brightness thresholding and complete segmentation, a finite group of sections, X1, X2, X3, etc., are visible in the image X.

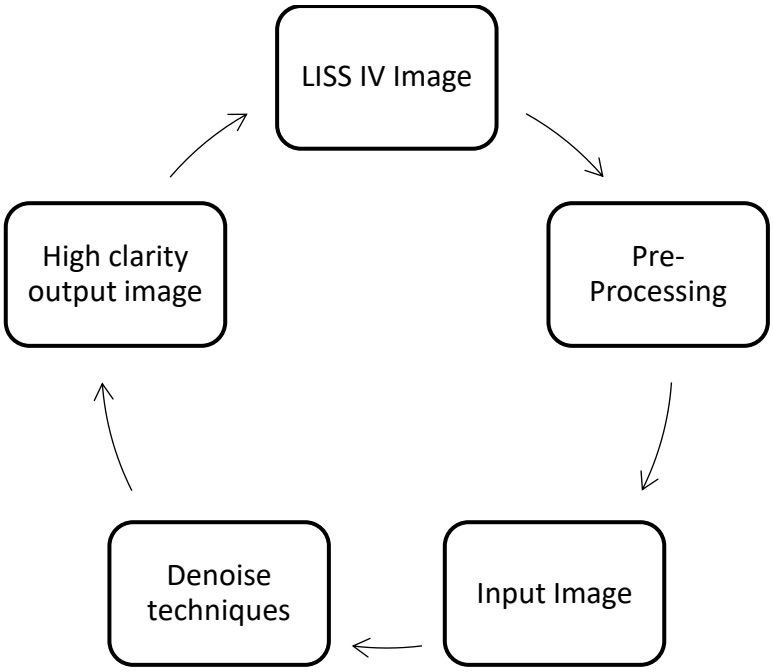

Figure 1. Steps for Image Enhancement

1.2. Edge Identification

The bulk of photos have far more complicated edge detection than the standard edge detection procedure for images [11][12]. Edge detection for aerial view photographs was possible, and computer vision camera captures of those things were also able to identify objects and detect edges, but edge detection for remote sensing images was significantly more challenging [13][14][15]. Locating the places in an image where there are discontinuities usually requires the use of edge detection techniques. Remote sensing photos with features like road areas, river floating, and building positions in grayscale, smoothing, equalized, threshold, and binary with OTSU conversion will benefit from the use of filters. in order to decide which edge detection filter is the most effective, it was suggested that the edge detection algorithms Sobel, Prewitt, Laplacian, and Canny be used to investigate the sample image [16][17][18]. Based on the value they receive; those filters offer the best results.

What makes edge detection essential? Edge boundaries of two regions were first segmented in order to identify the item in the image, and the original data from the image

was then erased. Determine the image classifications, such as smooth and sharp images [19][20], that will enable more precise object detection. If you want the greatest results, only this method will yield sharp photos. To locate the edges where there is a pronounced shift in intensity due to discontinuity, images must be interpreted as arrays containing samples of continuous functions of intensity [21]. Here, we'll take an example photo from a collection.

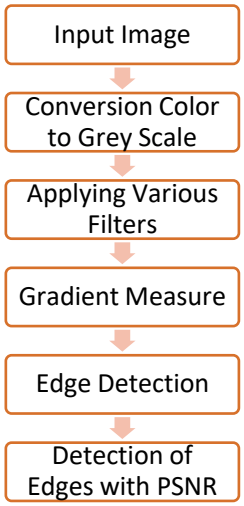

Figure 2. Process flow for edge detection

The edges in the remote sensing data were found using the suggested methods in this study, and the PSNR rate value was utilized to determine which PSNR rate value was best for the IRS P6 satellite image. [9] utilizing the Sobel operator to improve the edge extraction of quantum pictures while maintaining the essential elements. With this filter, it becomes more challenging to calculate the grey gradient accurately in terms of time and space. enhancing the edge by using threshold procedure. [10] This study has improved the edge detection technique for remote sensing photos by using genetic algorithms (GAs) to find the optimum Robert operator for 2D gradient measurement in high spatial resolution images.

1.2. Classification of Images

It has recently been shown that the high dimensionality of these data makes it difficult to pre-process them in a variety of ways. Utilizing a variety of learning strategies is one of the most crucial approaches to address this issue, according to recent studies. But if the data gets more complicated, existing approaches can no longer support it. The recommended approach illustrates that the maximum likelihood classifier may greatly reduce overfitting and obtain high classification accuracy by combining a variety of deep learning models, weight vector WV AdaBoost, and ADAM [22][23][24]. By recommending VGG16 and Inception v3, classification accuracy is increased and results at 96.08%.

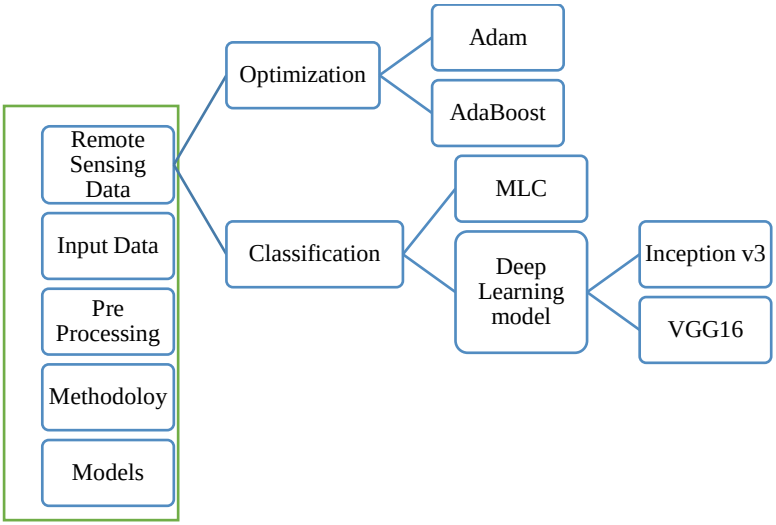

FIGURE 3. Pre-Processing steps.

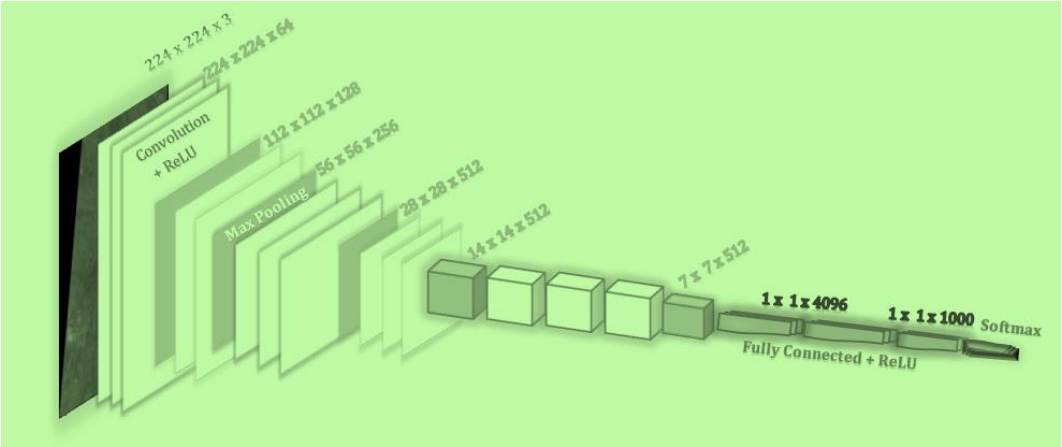

FIGURE 4: CNN Process Flow Model

2. Data and Methodology used

2.1. Data selection

We used IRS P6 LISS IV remote sensing data from ISRO for dataset analysis; for more information, go to https://directory.eoportal.org/web/eoportal/satellite-missions/i/irs-p6. The study only focuses on the Delhi region of India; it is situated at latitude 0.00000, longitude 75.00000, and the scene centre is at latitude 28.615513, longitude 77.216714, respectively. Table I, which also contains the combined RGB bands from Figure 8, provides a quick summary of the IRS P6 LISS IV data that we employed in our study.

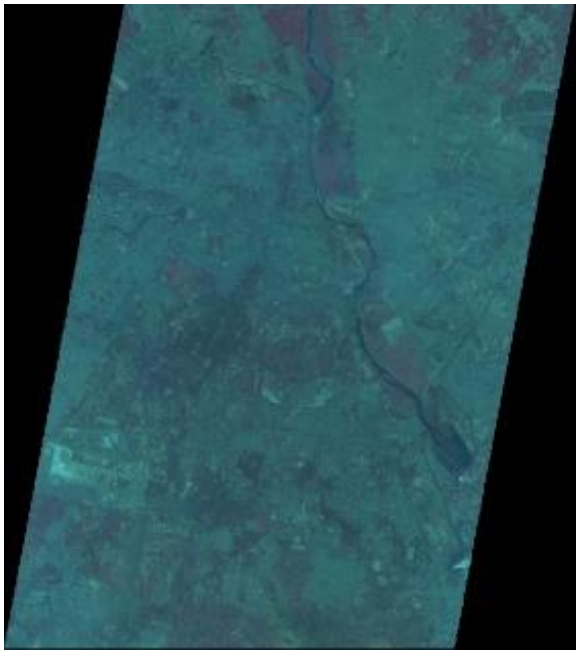

FIGURE 5. RGB combined band data.

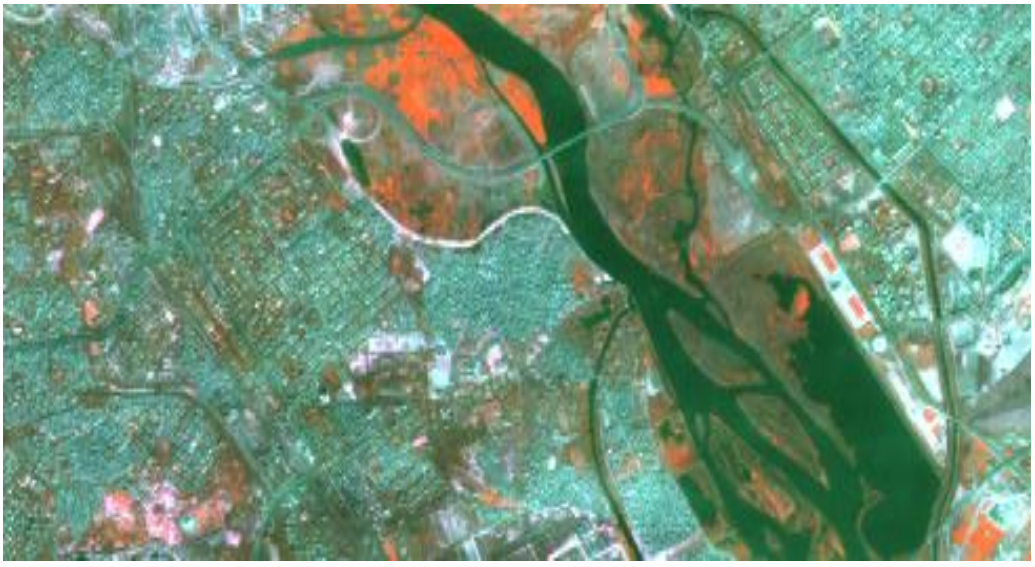

FIGURE 6. Vegetation area combined in a three-band image.

TABLE 1: Parameters Description

Parameter	Description
Parameter	LISS IV Data
Sensor	L4MX
Sat-ID	IRS-P6
Product ID	142866521
Sensor Orientation	Delhi
SAR Band	3 Band
Angle Range	Latitude 28.615513 Longitude 77.216714
Image Format	GEOTIFF
Range Resolution	5.8 m

In the table 1. mention of IRS Form P-6 Detailed description of the LISS IV data set.

3. Techniques and Results

3.1. Gaussian

Gaussian filter methods for enhancing contrast that use the frequency mechanism The use of linear filtering is substituted for nonlinear mapping approaches. Brightness is often adjusted to improvise contrast for the image. Noise reduction by the use of filters is homomorphic. The size of the kernel or matrix that will be used to demean the image is initially decided when a Gaussian filter is applied to a photograph [25][26]. The total results may be computed on the middle pixel because the sizes are usually odd integers. Due to their symmetry, the Kernels also have an equal number of rows and columns. The following describes the Gaussian function used to calculate the values within the kernel:

$$G(x,y) = \frac{1}{2\pi\sigma^2} e^{-\frac{x^2+y^2}{2\sigma^2}} \quad (1)$$

Where, x, y are coordinate values, constant PI value, σ Standard deviation.

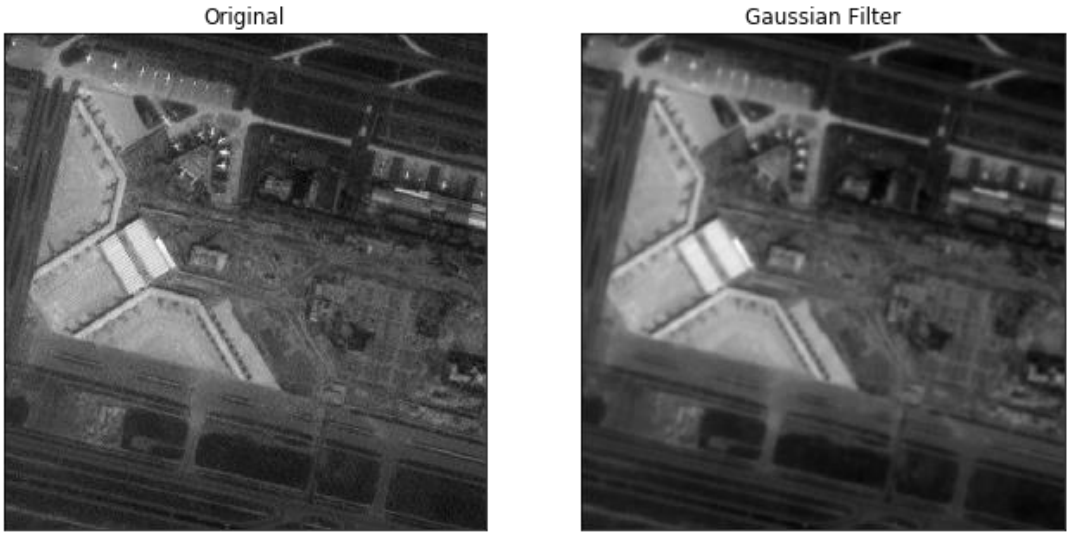

Figure 7. Enhancement of an image with a Gaussian filter

3.2. Algorithm for Canny Edge detection

The Canny edge detector, an edge detection operator, uses a multi-stage approach to recognize various edges in pictures. Using linear filtering with a Gaussian kernel, Canny edge detection calculates the edge intensity and direction for each pixel in the noise-smoothed picture [27][28]. Candidate edge pixels are identified by the non-maximal suppression thinning procedure that these pixels go through.

FIGURE 8. combined 3 band edge detection of the river zone and the vegetation

3.3. Performance indicators

$$PSNR = 10 \log 10 \frac{(2^n - 1)^2}{MSE} \quad (2)$$

$$MSE = \frac{\sum M,N \quad [I1(m,n) - I2(m,n)]2}{M * N} \quad (3)$$

Where 'I' is the intensity of the satellite image, which is zero in MSE (Eq. 3), and n is the number of bits in the grayscale image in PSNR (Eq. 1), M and N are rows and columns. A good and high-quality image delivers a higher PSNR value, where I1 stands for the intensity noise of the original, free image and I2 for a noisy image. By PSNR, a significant value was expected.

TABLE 2. Results of performance metrics Rate of PSNR

Techniques	Metric/ Source Fig number	Figure 9	Figure 10	Figure 11
Canny	**PSNR rate**	32.669	32.273	34.781

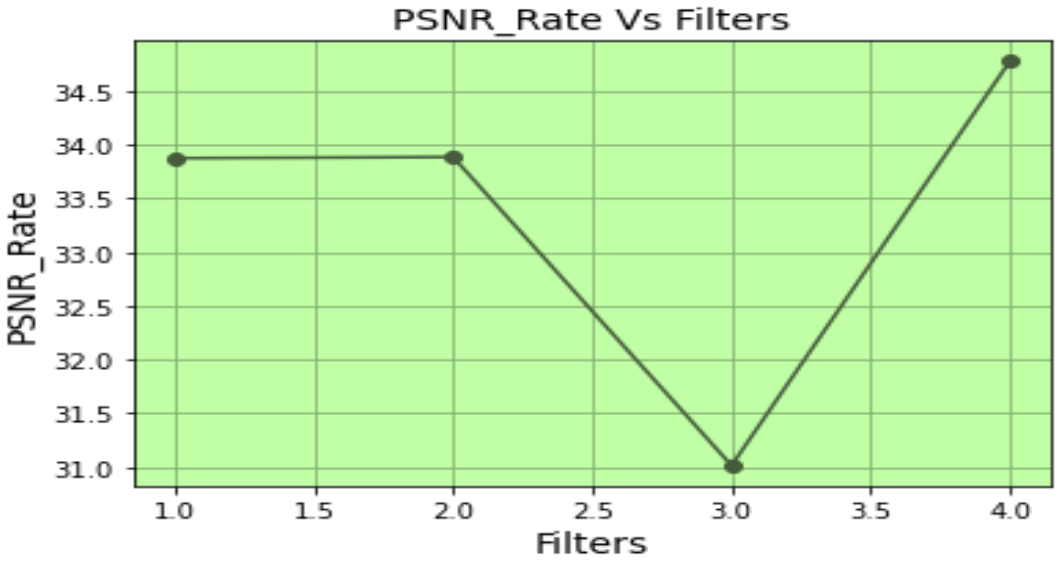

Figure 9. Performance chart for valuable metrics for clever results

3.4. Image classification algorithm techniques – Inception v3 Model

A deep convolutional neural network called Inception v3 was trained on the ImageNet data set for single-label picture categorization [29]. The TensorFlow team has already created a tutorial on how to retrain it to distinguish between various classes using our own examples. All of the model's layers will be used, with the exception of the last completely linked layer because it is unique to the ImageNet competition[30][31][32]. We flow the photos in batches of 20 using train datagen and test datagen after rescaling and applying Image Augmentation.

3.5. Vgg16 model

Convolutional neural network VGG16 was trained using data from a portion of the ImageNet dataset, which consists of approximately 866 actual class and correct class 835 categories. This model was proposed in the study, Very Deep Convolutional Networks for Large-Scale Image Recognition.

Table 3. Sample detail for the vegetation class of areas

Class No	Actual Class	Sample Used	Description
1	Veg Area-1		Forest area
2	Settle zone		Residential source area
3	River zone		River area

Table 4. Accuracy level of proposed model.

Class Name/ Type	Total No. of classes	Correct classes	Producer level accuracy %	User Level Accuracy %
1	283	260	97.97	91.77

2	331	326	93.68	98.51
3	252	249	99.7	98.22
Totals	866	835		

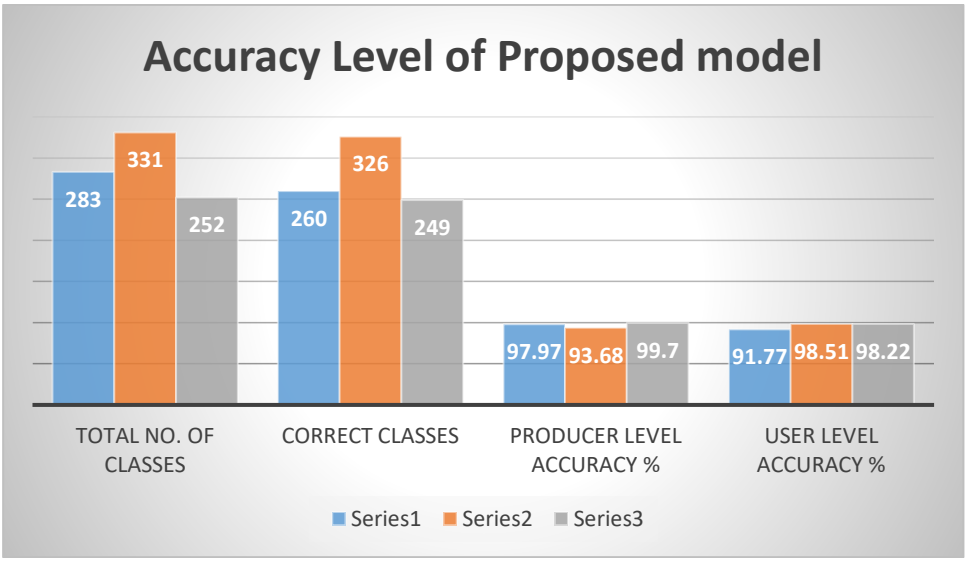

Figure 10. image classification accuracy level of proposed model

4. Conclusion and Future work

This research's primary goal is to analyze the multi-stage methods used on IRS p6 LISS IV remote sensing data. Generally, improve image clarity by mandating that enhancing techniques be used to the image data collection, followed by preprocessing and image scaling. To restore the image from distortion, it is necessary to apply noise and denoise to improve the image quality. Following this procedure, a better picture was captured for the canny filter's edge detection process, which generated a higher degree of image accuracy than the conventional filtering procedures. and used k means-clustering approaches to assess just the Inception v3 and vgg16 model for the picture classification step. The Python Jupyter Notebook's unsupervised image classification generates output results with producer level accuracy and user level accuracy of 99.7% in the type 3 class areas. Higher accuracy levels are produced by type 3, and producer level accuracy has grown relative to user level accuracy. The improvement test result was obtained by the research and analysis needed for testing and training using VGG16 and Inception v3 with Adam optimization.

Acknowledgments

Not applicable.

Competing Interests

The authors declare that they have no competing interests.

References

[1] *T.G. Kumar, D. Murugan, K. Rajalakshmi i T.I. Manish, "Image enhancement and performance evaluation using various filters for IRS-P6 Satellite Liss IV remotely sensed data", Geofizika, vol.32, br. 2, str. 179-189, 2015. [Online]. https://doi.org/10.15233/gfz.2015.32.11.*

[2] *Bajpai, K., & Soni, R. (2017). Analysis of Image Enhancement Techniques Used in Remote Sensing Satellite Imagery. International Journal of Computer Applications, 975, 8887.*

[3] *Lavania, K. K., & Kumar, R. (2012). Image enhancement using filtering techniques. International Journal on Computer Science and Engineering, 4(1), 14.*

[4] *Miljković, O. (2009). Image pre-processing tool. Kragujevac Journal of Mathematics, 32(32), 97-107..*

[5] *Deborah, H., & Arymurthy, A. M. (2010, December). Image enhancement and image restoration for old document image using genetic algorithm. In 2010 Second International Conference on Advances in Computing, Control, and Telecommunication Technologies (pp. 108-112). IEEE..*

[6] *Kaur, R., & Taqdir. (2016). Image Enhancement Techniques-A Review. International Research Journal of Engineering and Technology (IRJET), 3(3), 1308-1315.*

[7] *Bashir, I., Majeed, A., & Khursheed, O. (2017). Image restoration and the various restoration techniques used in the field of digital image processing. International Journal of Computer Science and Mobile Computing, 6(6), 390-393.*

[8] *Huang, S., Liu, Y., Wang, Y., Wang, Z., & Guo, J. (2020). A New Haze Removal Algorithm for Single Urban Remote Sensing Image. IEEE Access, 8, 100870-100889.*

[9] *A. A. Nayak, S. VenugopalaP., H. Sarojadevi, and N. N. Chiplunkar, "An Approach to Improvise Canny Edge Detection using Morphological Filters," Int. J. Comput. Appl., vol. 116, pp. 38–42, 2015.*

[10] *Y. Ma, H. Ma, and P. Chu, "Demonstration of Quantum Image Edge Extration Enhancement Through Improved Sobel Operator," IEEE Access, vol. 8, pp. 210277–210285, 2020, doi: 10.1109/ACCESS.2020.3038891.*

[11] *A. H. Abdel-Gawad, L. A. Said, and A. G. Radwan, "Optimized Edge Detection Technique for Brain Tumor Detection in MR Images," IEEE Access, vol. 8, pp. 136243–136259, 2020, doi: 10.1109/ACCESS.2020.3009898.*

[12] *M. Mittal et al., "An Efficient Edge Detection Approach to Provide Better Edge Connectivity for Image Analysis," IEEE Access, vol. 7, pp. 33240–33255, 2019, doi: 10.1109/ACCESS.2019.2902579.*

[13] *Q. Wu, F. Luo, P. Wu, B. Wang, H. Yang, and Y. Wu, "Automatic Road Extraction from High-Resolution Remote Sensing Images Using a Method Based on Densely Connected Spatial Feature-Enhanced Pyramid," IEEE J. Sel. Top. Appl. Earth Obs. Remote Sens., vol. 14, pp. 3–17, 2021, doi: 10.1109/JSTARS.2020.3042816.*

[14] *S. J. H. Pirzada and A. Siddiqui, "Analysis of edge detection algorithms for feature extraction in satellite images," in 2013 IEEE International Conference on Space Science and Communication (IconSpace), 2013, pp. 238–242, doi: 10.1109/IconSpace.2013.6599472.*

[15] *T. I. Manish, D. Murugan, and G. T. Kumar, "Hybrid edge detection using canny and ant colony optimization," Commun. Inf. Sci. Manag. Eng., vol. 3, no. 8, p. 402, 2013.*

[16] *X. Zhang and W. Zhang, "Application of New Multi-Scale Edge Fusion Algorithm in Structural Edge Extraction of Aluminum Foam," IEEE Access, vol. 8, pp. 15502–15517, 2020, doi: 10.1109/ACCESS.2019.2963454.*

[17] *Z. Zheng, B. Zha, H. Yuan, Y. Xuchen, Y. Gao, and H. Zhang, "Adaptive Edge Detection Algorithm Based on Improved Grey Prediction Model," IEEE Access, vol. 8, pp. 102165–102176, 2020, doi: 10.1109/ACCESS.2020.2999071.*

[18] *S. Janarthanan and K. Rajan, "Secure Efficient Geometric Range Queries on Encrypted Spatial Data," 2017.*

[19] *J. Shi, H. Jin, and Z. Xiao, "A Novel Hybrid Edge Detection Method for Polarimetric SAR Images," IEEE Access, vol. 8, pp. 8974–8991, 2020, doi: 10.1109/ACCESS.2020.2963989.*

[20] *R. Li, F. Tian, and S. Chen, "Research on Double Edge Detection Method of Midsole Based on Improved Otsu Method," IEEE Access, vol. 8, pp. 221539–221552, 2020, doi: 10.1109/ACCESS.2020.3043817.*

[21] *D. Wang, J. Yin, C. Tang, X. Cheng, and B. Ge, "Color Edge Detection Using the Normalization Anisotropic Gaussian Kernel and Multichannel Fusion," IEEE Access, vol. 8, pp. 228277–228288, 2020, doi: 10.1109/ACCESS.2020.3044341.*

[22] *M. Kalbasi and H. Nikmehr, "Noise-Robust, Reconfigurable Canny Edge Detection and its Hardware Realization," IEEE Access, vol. 8, pp. 39934–39945, 2020, doi: 10.1109/ACCESS.2020.2976860.*

[23] *X. Wang, J. Cao, Q. Hao, K. Zhang, Z. Wang, and S. Rizvi, "LBP-Based Edge Detection Method for Depth Images With Low Resolutions," IEEE Photonics J., vol. 11, no. 1, pp. 1–11, 2019, doi: 10.1109/JPHOT.2018.2884772.*

[24] *J. Chen, Z. Xi, C. Wei, J. Lu, Y. Niu, and Z. Li, "Multiple Object Tracking Using Edge Multi-Channel Gradient Model With ORB Feature," IEEE Access, vol. 9, pp. 2294–2309, 2021, doi: 10.1109/ACCESS.2020.3046763.*

[25] *C. Yao, Y. Kong, L. Feng, B. Jin, and H. Si, "Contour-Aware Recurrent Cross Constraint Network for Salient Object Detection," IEEE Access, vol. 8, pp. 218739–218751, 2020, doi: 10.1109/ACCESS.2020.3042203.*

[26] *Y. Peng, S. Ruan, G. Cao, S. Huang, N. Kwok, and S. Zhou, "Automated Product Boundary Defect Detection Based on Image Moment Feature Anomaly," IEEE Access, vol. 7, pp. 52731–52742, 2019, doi: 10.1109/ACCESS.2019.2911358.*

[27] *C. Wisultschew, G. Mujica, J. M. Lanza-Gutierrez, and J. Portilla, "3D-LIDAR Based Object Detection and Tracking on the Edge of IoT for Railway Level Crossing," IEEE Access, vol. 9, pp. 35718–35729, 2021, doi: 10.1109/ACCESS.2021.3062220.*

[28] *A. Ghorbanian and A. Mohammadzadeh, "An unsupervised feature extraction method based on band correlation clustering for hyperspectral image classification using limited training samples," Remote Sens. Lett., vol. 9, no. 10, pp. 982–991, 2018, doi: 10.1080/2150704X.2018.1500723.*

[29] *J. Song, S. Gao, Y. Zhu, and C. Ma, "A survey of remote sensing image classification based on CNNs," Big Earth Data, vol. 3, no. 3, pp. 232–254, 2019, doi: 10.1080/20964471.2019.1657720.*

[30] *A. K. Sharma, A. Gupta and S. Janarthanan, "Study on Information Management System that connects students and instructor through chatting," 2022 First International Conference on Artificial Intelligence Trends and Pattern Recognition (ICAITPR), 2022, pp. 1-5, doi: 10.1109/ICAITPR51569.2022.9844222.*

[31] *A. Gupta, H. K. Mall and S. Janarthanan., "Rainfall Prediction Using Machine Learning," 2022 First International Conference on Artificial Intelligence Trends and Pattern Recognition (ICAITPR), 2022, pp. 1-5, doi: 10.1109/ICAITPR51569.2022.9844203.*

[32] *Y. Wei, X. Luo, L. Hu, Y. Peng, and J. Feng, "An improved unsupervised representation learning generative adversarial network for remote sensing image scene classification," Remote Sens. Lett., vol. 11, no. 6, pp. 598–607, 2020, doi: 10.1080/2150704X.2020.1746854.*